

## Communications to the Editor

### Electrodeposition of Ordered Bi<sub>2</sub>Te<sub>3</sub> Nanowire Arrays

Amy L. Prieto,<sup>†</sup> Melissa S. Sander,<sup>†</sup>  
Marisol S. Martín-González,<sup>†</sup> Ronald Gronsky,<sup>‡</sup>  
Timothy Sands,<sup>‡</sup> and Angelica M. Stacy<sup>\*,†</sup>

Department of Chemistry  
University of California, Berkeley  
Berkeley, California

Department of Materials Science and Engineering  
University of California, Berkeley  
Berkeley, California 94720

Received April 10, 2001

Revised Manuscript Received June 4, 2001

Theoretical predictions suggest that the thermoelectric properties of nanowires will be enhanced significantly compared with bulk materials.<sup>1</sup> However, since a single nanowire does not have a high enough conductivity to be useful in most applications, it is necessary to use a template to organize a large collection of nanowires.<sup>2</sup> While there have been reports of the preparation of single nanowires of high quality, it is more challenging to fabricate arrays with a high density of nanowires ( $>5 \times 10^{10}$  nanowires/cm<sup>2</sup>) over a large area ( $>1$  cm<sup>2</sup>). As a step toward applying 1D thermoelectric materials, we have synthesized 40 nm diameter wires of Bi<sub>2</sub>Te<sub>3</sub> in porous alumina templates.

Bulk doped Bi<sub>2</sub>Te<sub>3</sub> is currently the most efficient thermoelectric material at 25 °C, and a good target material for thermoelectric nanowires. Prior work has shown that high-quality films of Bi<sub>2</sub>Te<sub>3</sub> can be deposited directly by electrochemical reduction of Bi<sup>3+</sup> and HTeO<sub>2</sub><sup>+</sup> in acidic aqueous solutions.<sup>3</sup> Wires with a diameter of ~250 nm have also been prepared by attaching a porous alumina template to a conducting material and confining the growth to within the pores.<sup>4</sup> Since the deposition occurs by electron transfer from the surface of the conducting material, the wires nucleate at the bottom of the pores and grow continuously up the pore. The fact that continuous wires are obtained is a key advantage of electrodeposition, particularly for applications in which conductivity is important (e.g., thermoelectric devices). In addition, porous alumina is a good choice for a template because the pore diameters are easily adjusted (down to 9 nm) to sizes enabling quantum confinement. Moreover, the pore densities (~7

$\times 10^{10}$  pores/cm<sup>2</sup>) and aspect ratios (up to 100  $\mu$ m long) are high.<sup>5</sup> We have therefore extended prior work on electrodeposition into porous alumina to fabricate nanoscale Bi<sub>2</sub>Te<sub>3</sub> wires. In this work, we describe conditions (solution concentrations, potentials, temperature, and template thickness) that yield dense wires with the desired composition and morphology. The diameters are small enough to anticipate both quantum confinement and enhanced thermoelectric response.

The fabrication of 40 nm porous alumina templates was adapted from several sources.<sup>6</sup> Aluminum foil (Alfa Aesar, 4 cm<sup>2</sup>, 0.13 mm thick, 99.9995%) was polished mechanically and electrochemically and then anodized in 4 wt % oxalic acid (2 °C) at 30 V for 20 to 50 h, depending on the desired thickness. This process yielded films of porous Al<sub>2</sub>O<sub>3</sub> between 30 and 80  $\mu$ m thick with 40 nm diameter pores. Approximately 1  $\mu$ m of Ag was sputter-deposited (Perkin-Elmer Randex 2400) on the top face of the template to serve as the conducting surface of the electrode. The Al foil/alumina/Ag composite was soaked in a saturated HgCl<sub>2</sub> solution to remove the remaining Al from the bottom side. The barrier layer of Al<sub>2</sub>O<sub>3</sub> just above the Al was removed by dissolution with a saturated solution of KOH in ethylene glycol.

Electrodeposition of Bi<sub>2</sub>Te<sub>3</sub> was performed using a standard three-electrode cell (EG&G PAR model 273 potentiostat/galvanostat). Copper wire was attached to the Ag side of the porous alumina template with Ag paint (Ted Paella, Inc., colloidal silver paste), and the back and edges of the alumina were masked with clear nail enamel. The cathode assembly (porous alumina with Ag) and anode (Pt gauze) were submerged in a solution of 1 M HNO<sub>3</sub>, which was used to dissolve varying amounts of elemental Bi (Mallinckrodt, 99.8%), and Te (Alfa Aesar, 99.9998%). The reference electrode (Hg/Hg<sub>2</sub>SO<sub>4</sub>) was in a separate cell in a 1 M KNO<sub>3</sub> solution. The two cells were connected via a 1 M KNO<sub>3</sub>/agar salt bridge. Depositions of Bi<sub>2</sub>Te<sub>3</sub> were performed under potentiostatic control with potentials more negative than -0.45 V versus Hg/Hg<sub>2</sub>SO<sub>4</sub>.

Even under a range of electrodeposition conditions, nanowire composition, as determined by energy dispersive spectroscopy performed in a scanning electron microscope (JEOL 6300), remained constant at 40 atomic % Bi and 60 atomic % Te ( $\pm 5\%$ ) as expected for Bi<sub>2</sub>Te<sub>3</sub>. A powder X-ray diffraction pattern (Siemens D5000 Diffractometer, Cu K $\alpha$  radiation) for the product Bi<sub>2</sub>Te<sub>3</sub>/Al<sub>2</sub>O<sub>3</sub> composite, shown in Figure 1, compares well to the known pattern for Bi<sub>2</sub>Te<sub>3</sub> (Powder Diffraction File 82-0358). All peaks can be indexed to the rhombohedral space group  $R\bar{3}m$ , except the broad low-angle bulge, which is due to the amorphous Al<sub>2</sub>O<sub>3</sub> template.

The 110 peak is larger than expected for a random polycrystalline sample, indicating strong texturing. The wire axis is [110], which means that the Bi<sub>2</sub>Te<sub>3</sub> cleavage planes are perpendicular to the Ag surface. This is the optimal orientation for the thermoelectric properties of Bi<sub>2</sub>Te<sub>3</sub>. Since the electrical conductivity perpendicular to the 110 planes is the highest, it is not surprising that the wires grow preferentially in this direction. Annealing at 500 °C for one week further increases the relative intensity of the 110 peak as expected from grain coarsening.

(5) Shingubara, S.; Okino, O.; Sayama, Y.; Sakaue, H.; Takahagi, T. *Jpn. J. Appl. Phys.* **1997**, *36*, 7791.

(6) (a) Miller, C. *Microporous Aluminum Oxide Films at Electrodes*; University of California, Berkeley: Berkeley, 1987, 271. (b) Zhang, Z.; Gekhtman, D.; Dresselhaus, M. S.; Ying, J. Y. *Chem. Mater.* **1999**, *11*, 1659. (c) Keller, F.; Hunter, M. S.; Robinson, D. L. *J. Electrochem. Soc.* **1953**, *100*, 411.

\* To whom correspondence should be addressed.

<sup>†</sup> Department of Chemistry.

<sup>‡</sup> Department of Materials Science and Engineering.

(1) (a) Hicks, L. D.; Dresselhaus, M. S. *Phys. Rev. B* **1993**, *47*, 12727. (b) Hicks, L. D.; Dresselhaus, M. S. *Phys. Rev. B* **1993**, *47*, 16631. (c) Hicks, L. D.; Harman, T. C.; Sun, X.; Dresselhaus, M. S. *Phys. Rev. B* **1996**, *53*, 10493. (d) Harman, T. C.; Spears, D. L.; Walsh, M. P. *J. Electron. Mater.* **1999**, *28*, L1. (e) Harman, T. C.; Spears, D. L.; Manfra, M. J. *J. Electron. Mater.* **1996**, *25*, 1121. (f) Koga, T.; Harman, T. C.; Cronin, S. B.; Dresselhaus, M. S. *Phys. Rev. B* **1999**, *60*, 14286. (g) Harman, T. C.; Taylor, P. J.; Spears, D. L.; Walsh, M. P. *J. Electron. Mater.* **2000**, *29*, L1. (h) Venkatasubramanian, R.; Colpitts, T.; Watko, E.; Hutcheon, J. *IEEE 15th Int. Conf. Thermoelectrics* **1996**, 454. (i) Cho, S.; DiVenere, A.; Wong, G. K.; Ketterson, J. B.; Meyer, J. R. *Phys. Rev. B: Condens. Matter* **1999**, *59*, 10691. (j) Broido, D. A.; Reinecke, T. L. *Appl. Phys. Lett.* **1995**, *67*, 100.

(2) (a) Martin, C. R. *Adv. Mater.* **1999**, *3*, 457. (b) Martin, C. R. *Science* **1994**, *266*, 1961.

(3) (a) Takahashi, M.; Oda, Y.; Ogino, T.; Furuta, S. *J. Electrochem. Soc.* **1993**, *140*, 2550. (b) Takahashi, M.; Katou, Y.; Nagata, K.; Furuta, S. *Thin Solid Films* **1994**, *240*, 70. (c) Magri, P.; Boulanger, C.; Lecuire, J. M. In *Electrodeposition of Bi<sub>2</sub>Te<sub>3</sub> Films*; Mathiprakasham, B., Heenan, P., Ed.; AIP Press: Kansas City, 1994; p 277. (d) Magri, P.; Boulanger, C.; Lecuire, J. M. *J. Mater. Chem.* **1996**, *6*, 773.

(4) Sapp, S. A.; Lakshmi, B. B.; Martin, C. R. *Adv. Mater.* **1999**, *11*, 402.

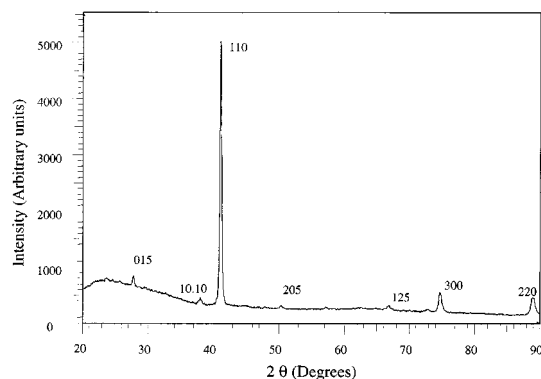


**Figure 1.** Representative X-ray diffraction pattern of a filled 40 nm template. The high intensity of the 110 peak indicates preferred orientation; the wire axis is [110].

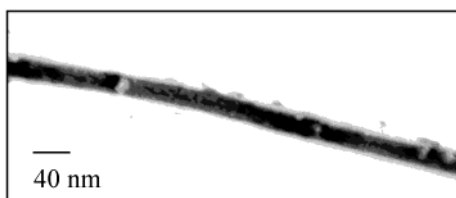


**Figure 2.** Bright-field TEM image of a single  $\text{Bi}_2\text{Te}_3$  nanowire. The image shows that the wire is continuous, dense, and highly crystalline.

To probe the crystallinity of the as-deposited nanowires further, the alumina matrix was dissolved selectively by soaking the templates in a solution of 3.5 vol %  $\text{H}_3\text{PO}_4$  and 45 g/L  $\text{CrO}_3$  for approximately 1 day. A bright-field image of a single  $\text{Bi}_2\text{Te}_3$  nanowire taken in a transmission electron microscope (JEOL 200CX) is shown in Figure 2. Analysis of several individual wires, both by imaging and electron diffraction, indicate that the wires are dense, continuous, and highly crystalline.

While we have been able to obtain high-quality single wires by direct electrodeposition, the fabrication of arrays with a high degree of pore filling is significantly more challenging. During depositions, we observed that the current remains fairly constant as the pores are filling. Once growth occurs laterally across the top surface, there is a steady increase in the current due to the enlargement of the cathode area on which  $\text{Bi}_2\text{Te}_3$  is depositing. The templates gradually turn black in the regions where there is filling. In the best cases, the current remains constant over at least 12–14 h for a 60  $\mu\text{m}$  thick template, and the templates are uniformly black after this time. However, only 10–20% of the pores are filled completely.

Several factors affect the degree of pore filling. First, pore-to-pore variations in nucleation rate arise from the presence of heterogeneities at the cathode interface, such as grain boundaries or adsorbed impurities. Since the exposed cathodic surface area at the bottom of each 40 nm diameter pore is only  $\sim 1300 \text{ nm}^2$ , very small quantities of impurities can completely suppress nucleation of a wire. Second, even if wires are nucleated in all the pores, the rate of growth must be uniform so that all wires grow to the length of the pore simultaneously. If a few pores fill rapidly with  $\text{Bi}_2\text{Te}_3$ , then growth continues laterally across the top surface, closing off unfilled pores in the process. Third, if there are very small cracks in the alumina, even slightly larger than the pore diameter (in this case, 40 nm), deposition will occur predominantly in the cracks due to greater accessibility of cations.<sup>7</sup>

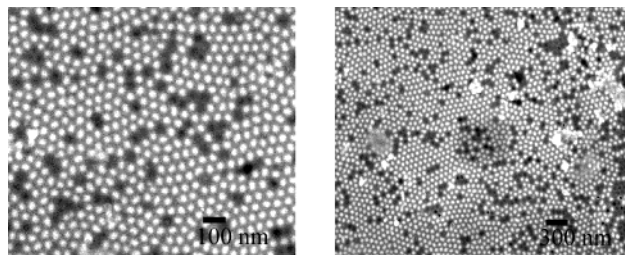


**Figure 3.** SEM image of  $\text{Bi}_2\text{Te}_3$  nanowire array composite. The bright regions are the filled pores. EDS of the surface of the samples shows 40 atomic % Bi; 60 atomic % Te.

To enhance reproducibility and degree of pore filling, we have examined the choice of electrode material, the rate of deposition, and the thickness of the alumina templates. By using Pt as a cathode, potentials more negative than  $-0.65 \text{ V}$  versus  $\text{Hg}/\text{Hg}_2\text{SO}_4$ , and  $\sim 100 \mu\text{m}$  thick templates, we observed nucleation in 65–75% of the pores, but only in small regions of the templates. To nucleate wires in as many pores as possible, we instead chose Ag as the cathode because cyclic voltammetry studies indicate that there is a strong interaction between chalcogenides and Ag.<sup>8</sup> This interaction should favor nucleation. To grow wires simultaneously in as many pores as possible, we tried to minimize the rate of growth by reducing the concentrations of Bi and Te to  $\sim 1 \times 10^{-2} \text{ M}$  (until the limit where  $\text{H}_2$  begins to be evolved), by employing the least negative deposition potential ( $-0.45 \text{ vs Hg}/\text{Hg}_2\text{SO}_4$ ), and by lowering the temperature to  $\sim 2 \text{ }^\circ\text{C}$ . To avoid excessive cracking in the alumina templates while maintaining structural integrity, we used templates with a thickness of  $\sim 50 \mu\text{m}$ .

While we have not yet achieved 100% pore filling and reproducibility is not high, we have been able to nucleate wires in up to 80% of the pores throughout the templates. Scanning electron micrographs (JEOL 6300) of the bottom surface of a nanowire array prepared under optimized conditions are shown in Figure 3. The array was polished to remove  $\text{Bi}_2\text{Te}_3$  from the top surface and the Ag cathode from the backside to reveal the alumina template filled with  $\text{Bi}_2\text{Te}_3$ . While only  $\sim 20\%$  of the pores are completely filled, wires have nucleated in  $>80\%$  of the pores.

In summary, we have demonstrated the fabrication of dense, continuous  $\text{Bi}_2\text{Te}_3$  wires with uniform diameters of 40 nm by direct electrodeposition into an alumina template. The deposited wires are highly textured in the [110] direction. Furthermore, with a template that is  $\sim 50 \mu\text{m}$  thick, a sputtered Ag cathode, and a current density of  $\sim 1 \text{ mA}/\text{cm}^2$ , nanowire yield in  $>80\%$  of the pores has been obtained. We conclude that direct electrodeposition into nanoporous alumina templates can be used for the fabrication of nanowire arrays as required for implementation in devices.

**Acknowledgment.** Funding for this work was provided by the Department of Defense ONR-MURI on Thermoelectrics, N00014-97-1-0516. We thank R. Wilson (Department of Materials Science, UCB) for help with the SEM/EDS data, Professor J. Long (Department of Chemistry, UBC) for the use of the Bioanalytical Systems Basomatic CV50W, and Dr. J.-P. Fleurial, Dr. G. J. Snyder, and Dr. A. Borchshevsky (JPL) for helpful discussions. A.L.P. thanks Lucent Technologies, Bell Labs for funding.

JA015989J

(7) Routkevitch, D.; Bigioni, T.; Moskovits, M.; Ming Xu, J. *J. Phys. Chem.* **1996**, *100*, 14037.

(8) Foresti, M. L.; Pezzatini, G.; Cavallini, M.; Aloisi, G.; Innocenti, M.; Guidelli, R. *J. Phys. Chem. B* **1998**, *102*, 7413.